Research

Authors for correspondence:
Alina Glaubitz
e-mail: alina.glaubitz.gr@dartmouth.edu
Feng Fu
e-mail: feng.fu@dartmouth.edu

Oscillatory dynamics in the dilemma of social distancing

Alina Glaubitz[1] and Feng Fu[1,2]

[1]Department of Mathematics, Dartmouth College, Hanover, NH 03755, USA
[2]Department of Biomedical Data Science, Geisel School of Medicine at Dartmouth, Lebanon, NH 03756, USA

AG, 0000-0001-9609-3712; FF, 0000-0001-8252-1990

Social distancing as one of the main non-pharmaceutical interventions can help slow down the spread of diseases, like in the COVID-19 pandemic. Effective social distancing, unless enforced as drastic lockdowns and mandatory cordon sanitaire, requires consistent strict collective adherence. However, it remains unknown what the determinants for the resultant compliance of social distancing and their impact on disease mitigation are. Here, we incorporate into the epidemiological process with an evolutionary game theory model that governs the evolution of social distancing behaviour. In our model, we assume an individual acts in their best interest and their decisions are driven by adaptive social learning of the real-time risk of infection in comparison with the cost of social distancing. We find interesting oscillatory dynamics of social distancing accompanied with waves of infection. Moreover, the oscillatory dynamics are dampened with a non-trivial dependence on model parameters governing decision-makings and gradually cease when the cumulative infections exceed the herd immunity. Compared to the scenario without social distancing, we quantify the degree to which social distancing mitigates the epidemic and its dependence on individuals' responsiveness and rationality in their behaviour changes. Our work offers new insights into leveraging human behaviour in support of pandemic response.

1. Introduction

Emerging novel zoonotic diseases, such as Zika [1], Ebola [2] and the most recently COVID-19 [3], have

imposed great threats to global health and humanity [4]. Some of these new diseases are caused by respiratory viruses and highly contagious through proximity transmissions, and may turn into an unprecedented pandemic well before effective treatments and vaccines have been developed and widely deployed. In this case, the world may have to resort to non-pharmaceutical interventions (NPI), such as face covering and social distancing so as to mitigate disease impact before effective pharmaceutical interventions become available. However, the ultimate effectiveness of NPI measures is highly contingent on compliance and adherence, since NPI is usually not a one-off measure, but rather requires repeated, consistent adherence in order to reduce potential transmission routes of contracting the infection. From this perspective, human behaviour plays an important role in impacting the course of a pandemic outbreak as well as the health outcome.

In recent years, there has been growing interest in understanding social factors in epidemiology (see, for example, [5] for a brief review). In the field of behavioural epidemiology, of particular interest is the use of disease-behaviour interaction models for this purpose [6]. Prior work has extensively used this framework to study how vaccine compliance can be influenced by a wide range of factors [7–9], ranging from vaccine scares [10] to disease awareness [11]. The feedback loop between behavioural change and disease prevalence gives rise to a variety of interesting, non-trivial dynamics [12–15], e.g. the hysteresis effect [16]. Among others, an important approach is combining evolutionary game theory with epidemiological models [7, 17,18]. Evolutionary game theory provides a general mathematical framework for modelling behavioural changes in a population driven by both social influence and self-interest. In the past decades, the approach of replicator dynamics has been commonly used to model social learning/imitation process, and particularly the spread of behaviour (social contagion), in a range of important real-world problems [19], from peer punishment [20] over cooperation [21], altruistic punishment [22], honesty [23], trust [24] and moral behaviour in general [25] to antibiotic usage [26].

Unlike vaccination, social distancing effort of an individual requires repeated decisions whether or not to comply by evaluating the necessity of doing so throughout the epidemic, despite public health recommendations or even mandates [27]. The cost of social distancing is not negligible, but rather has a huge impact on the economic status and well-being of people [28]. Previous work has modelled social distancing as a differential game [29], that is, individuals try to maximize their payoffs by adjusting their effort in social distancing (namely, the level of exposure to potential transmission routes) by comparing the risk of contracting the disease with the cost of social distancing. Their numerical results show that the collective dynamics of social distancing would approach to a steady level (i.e. a Nash equilibrium with constant effort for social distancing) without any oscillatory dynamics [29]. While this prior study sheds useful insights for social distancing from the game theory perspective, it remains largely unknown how the rationality and the responsiveness of individuals in reacting to an epidemic would impact the compliance level of social distancing.

Social distancing is costly, yet if not optimized for timing and duration and intensity, it would lead to wasted effort [30,31]. Combined with real data, the impact of social distancing can also be quantitatively assessed and optimized for past pandemics like influenza [32,33]. Noteworthy, there have been efforts to predict and quantify the effectiveness of reactive distancing on the COVID-19 pandemic, in anticipation of multiple waves of infections in the coming years [34,35].

Aside from individual perspective, the optimization of disease control is often studied using optimal control theory by assuming a central social planner aiming to minimize the cost of disease outbreak [36–39]. While these results are insightful from the perspective of population optima [40] (that is, optimized policies are complied uniformly in the population), it is challenging to attain these goals in practice due to compliance issues.

To shed light on driving factors of compliance levels of social distancing, here we take into account important aspects of human decision-making—bounded rationality [41] and loss aversion [42]—which is informed by the real-time disease prevalence, and prompted by peers' choice. We incorporate into the epidemiological process with an evolutionary game dynamics of social distancing behaviour. Individuals decide on whether or not to commit to social distancing

by weighing the risk of infection with the cost of social distancing. The responsiveness parameter in our model modulates the relative time scale of individuals revisiting their social distancing decisions, as compared to the pace of an unfolding epidemic. We introduce bounded rationality that individuals are not necessarily using the best response but rather with some probability of changing their behaviour.

In this work, we find an interesting *oscillatory tragedy of the commons* in the collective dynamics of social distancing. Individuals are inclined to social distancing when the disease prevalence is above a threshold that depends on the transmissibility of the disease and the relative cost of social distancing versus contracting the disease. As the epidemic curve is being flattened, individuals consequently feel more safe not to practise social distancing, thereby causing the decline in the compliance of social distancing and further resulting in a resurgence of disease outbreaks in the population. Even though such reactive social distancing is hardly able to help reach the optimality of disease mitigation, it can avoid the overshooting of infected individuals which typically happens in an susceptible–infected–recovered (SIR) model in the absence of any interventions. We also find non-trivial dependence of the effectiveness of social distancing, measured by the fraction of susceptible individuals who would become infected without social distancing, on model parameters governing individuals' rationality and responsiveness.

2. Model and methods

(a) Model

Our model is basically a combination of the classical SIR model with the replicator equation: In a well-mixed infinite population each individual is either susceptible, infected or recovered. Moreover, each susceptible individual can at each time choose to either practise social distancing or not to practise social distancing. If the individual practises social distancing they cannot become infected. If they do not practise social distancing they become infected in an encounter with an infected individual with probability $\beta > 0$. At each time an infected recovers with probability $\gamma > 0$ (figure 1).

We denote the proportion of susceptible individuals at time t by $S(t)$, the proportion of infected by $I(t)$, and the proportion of removed by $R(t)$. Furthermore, we denote by $\mathcal{E}(t)$ the proportion of susceptible individuals that practise social distancing. We denote the initial conditions by $I_0 = I(0), S_0 = S(0)$ as well as $\mathcal{E}_0 = \mathcal{E}(0)$. A susceptible individual determines his strategy based on a cost-benefit analysis. Hence, by π_{sd} we denote the payoff of social distancing, and by π_{nsd} the payoff of no social distancing. In our model, the perceived cost of social distancing is $C_{sd} > 0$ at each time t. Thus, we have
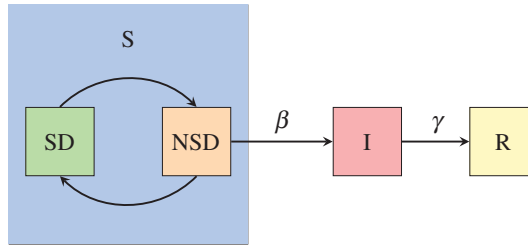
$$\pi_{sd} = -C_{sd}.$$

π_{nsd} depends on two factors: the perceived cost of infection that we denote by $C_I > 0$ and the risk of infection. The risk of infection in time $(t, t+1)$ without social distancing is given by

$$1 - \exp\left(-\beta \int_t^{t+1} I(\tau)\, d\tau\right) \approx 1 - \exp\left(-\beta I(t)\right).$$

Therefore, the payoff of not socially distancing is given by

$$\pi_{nsd} = -C_I(1 - \exp\left(-\beta I(t)\right)).$$

Figure 1. Schematic of our model. In contrast to the SIR model, we divide the susceptible population into those that practise social distancing (and cannot be infected) and those that do not practise social distancing (and can be infected). The dynamics of the amount of people practising social distancing is given by a replicator equation. Here as well as in later figures, we refer to those practising social distancing as SD and those that do not as NSD. (Online version in colour.)

Hence, the dynamics of our model are given by the following system of ordinary differential equations (ODEs):

$$\begin{aligned}
\dot{S}(t) &= -\beta(1 - \mathcal{E}(t))S(t)I(t) \\
\dot{I}(t) &= \beta(1 - \mathcal{E}(t))S(t)I(t) - \gamma I(t) \\
\dot{R}(t) &= \gamma I(t) \\
\dot{\mathcal{E}}(t) &= \omega\mathcal{E}(t)(1 - \mathcal{E}(t))\tanh\left(\frac{\kappa}{2}\left(-C_{sd} + C_I\left(1 - e^{-\beta I(t)}\right)\right)\right).
\end{aligned} \qquad (2.1)$$

and

Here, ω is a responsiveness parameter, determining the time scale for updating the social distancing behaviour. κ is a rationality parameter. For large κ individuals change their strategy if the payoff of the other strategy is larger. For small κ only a fraction of the susceptible individuals depending on the difference in payoff change their strategy. The behaviour of this model is illustrated in figure 2 for different parameters. For this figure as well as for all other figures, we used the Matlab method ode23, which is an implementation of the Bogacki–Shampine method—an explicit Runge–Kutta (2,3) pair.

(b) Perfect adaption

In Model (2.1), the dynamics of social distancing $\mathcal{E}$ change to direct the amount of infected I towards the amount where $\pi_{sd} = \pi_{nsd}$, i.e. towards I^*. Assuming that this adaption works perfectly, we obtain the following model given by the ODEs.

This model is given by the ODEs

$$\dot{I}_{PA}(t) = \begin{cases} 0, & t < t^* \\ \beta I(t)S(t) - \gamma I(t), & t > t^* \end{cases} \qquad (2.2)$$

and

$$\dot{R}_{PA}(t) = \gamma I(t)$$

with $S(t) = 1 - I_{PA}(t) - R_{PA}(t)$, $t^* = -(\gamma - \beta + \beta I^*)/\beta I^* \gamma$, and with initial condition
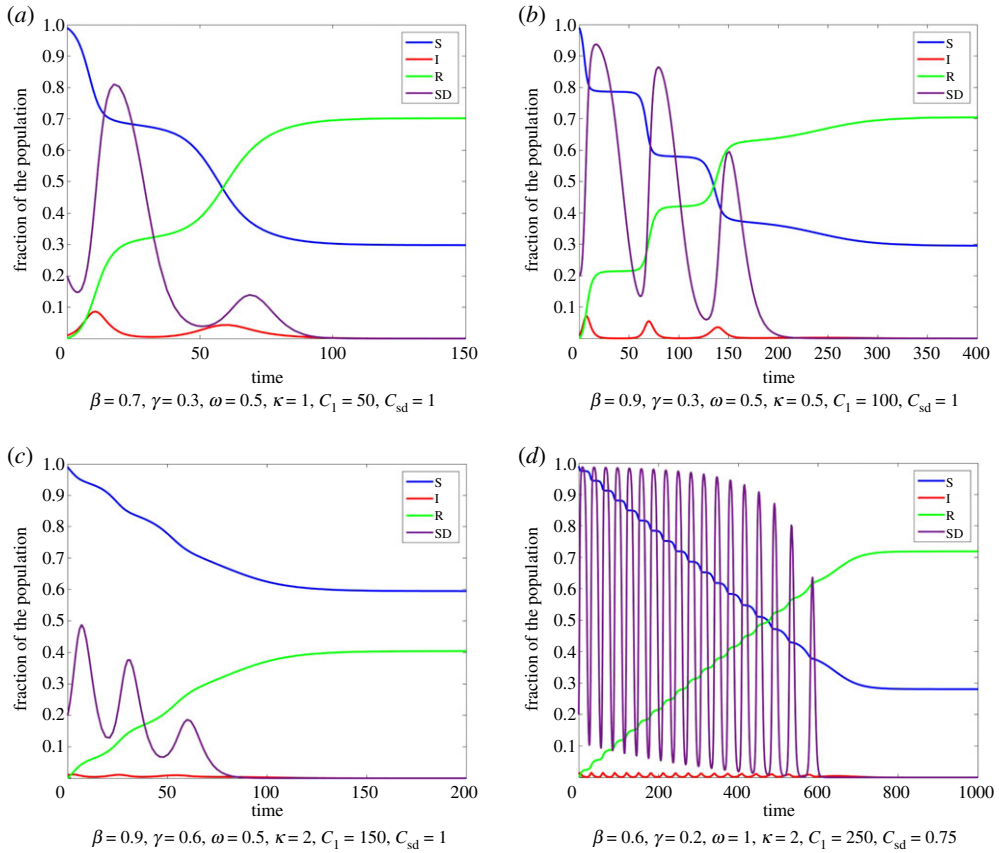
$$I_{PA}(0) = I^*, \qquad R_{PA}(0) = 0.$$

An illustration of this model is given in figure 3.

Then, the total amount of people that get infected $R_{PA}(\infty)$ is given by

$$R_{PA}(\infty) = \frac{\gamma}{\beta}W\left(-\exp\left(-\frac{I^*\beta}{\gamma} - 1\right)\right) + 1,$$

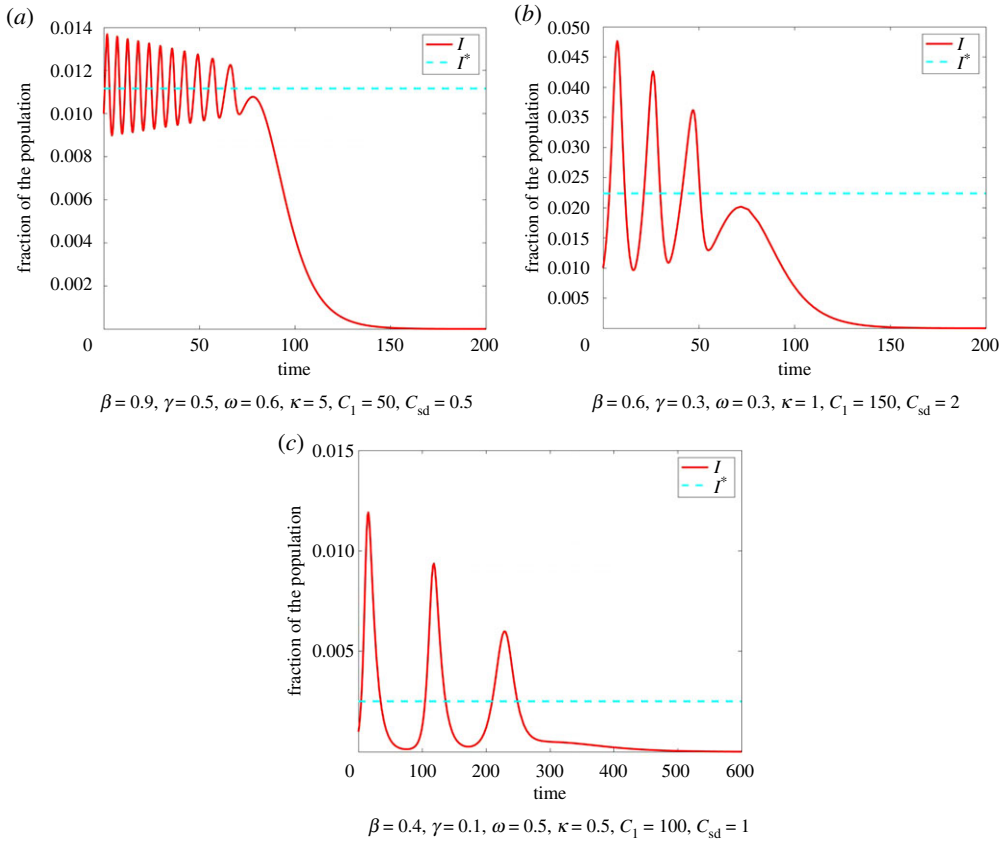where W denotes the Lambert W function. Thus, in the case of perfect adaption, we can achieve

$$R_{PA}(\infty) \to 1 - \frac{\gamma}{\beta}$$

5

royalsocietypublishing.org/journal/rspa   *Proc. R. Soc. A* **476**: 20200686

Figure 2. Model (2.1) for different parameters with $I_0 = 0.01$, $S_0 = 0.99$, $\mathcal{E}_0 = 0.2$. SD Here, as well as for all other figures, we used the Matlab method ode23, which is an implementation of the Bogacki–Shampine method—an explicit Runge–Kutta (2,3) pair. (Online version in colour.)
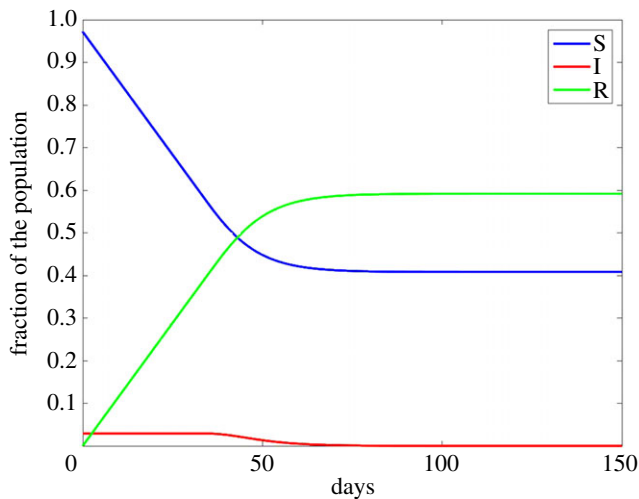
Figure 3. Perfect adaptation with $\beta = 0.7$, $\gamma = 0.4$, $C_d = 0.75$, $C_l = 50$. Here, $I(t) = I^*$ until herd immunity occurs, i.e. $S < \gamma/\beta$. From that point on, the model is a classical SIR model with $I_0 = I^*$, $R_0 = \gamma I^* t^* = 1 - \gamma/\beta - I^*$. (Online version in colour.)

6

royalsocietypublishing.org/journal/rspa Proc. R. Soc. A **476**: 20200686

(*a*)

$\beta = 0.9,\ \gamma = 0.5,\ \omega = 0.6,\ \kappa = 5,\ C_1 = 50,\ C_{sd} = 0.5$

(*b*)

$\beta = 0.6,\ \gamma = 0.3,\ \omega = 0.3,\ \kappa = 1,\ C_1 = 150,\ C_{sd} = 2$

(*c*)

$\beta = 0.4,\ \gamma = 0.1,\ \omega = 0.5,\ \kappa = 0.5,\ C_1 = 100,\ C_{sd} = 1$

Figure 4. Oscillations of the number of infected around I^* in Model (2.1) with initial condition $I_0 = 0.01$, $S_0 = 0.99$, $\mathcal{E}_0 = 0.3$. In each instance, I oscillates around I^* with decreasing amplitude until the peak is smaller than I^*. We see that the number and amplitude of oscillations depends on the parameters $\omega, \kappa, C_{sd}, C_I$ as well as β and γ. (Online version in colour.)

by choosing $C_{\dot{a}}/C_I \to 0$. We want to use this model of perfect adaption to understand how the total amount of infected $R(\infty)$ in Model (2.1) depends on the parameters $C_{sd}, C_I, \omega, \kappa$.

3. Results

(a) Oscillatory tragedy of the commons

In Model (2.1), the cost of social distancing and no social distancing are equal at time t if

$$I(t) = I^* := -\frac{1}{\beta} \log\left(1 - \frac{C_{sd}}{C_I}\right).$$

If $I > I^*$, then $\mathcal{E}$ is increasing. If $I < I^*$ then $\mathcal{E}$ is decreasing. On the other hand, if $\mathcal{E}$ is sufficiently large, this causes a decrease in I and if $\mathcal{E}$ is sufficiently small this causes an increase in I. If the amount of infections is high, people are more aware of the disease and practise social distancing. As soon as the amount of infections is small again, this awareness fades and people do not feel the need to practise social distancing anymore. As a result, more people become infected again leading to a higher awareness and more people practising social distancing. We refer to this feedback loop as *oscillatory tragedy of the commons*. Instead of high compliance to social distancing until the disease has died of, we find a decrease in individuals practising social distancing when the amount of infected is sufficiently small. This then causes another rise of infections. We can
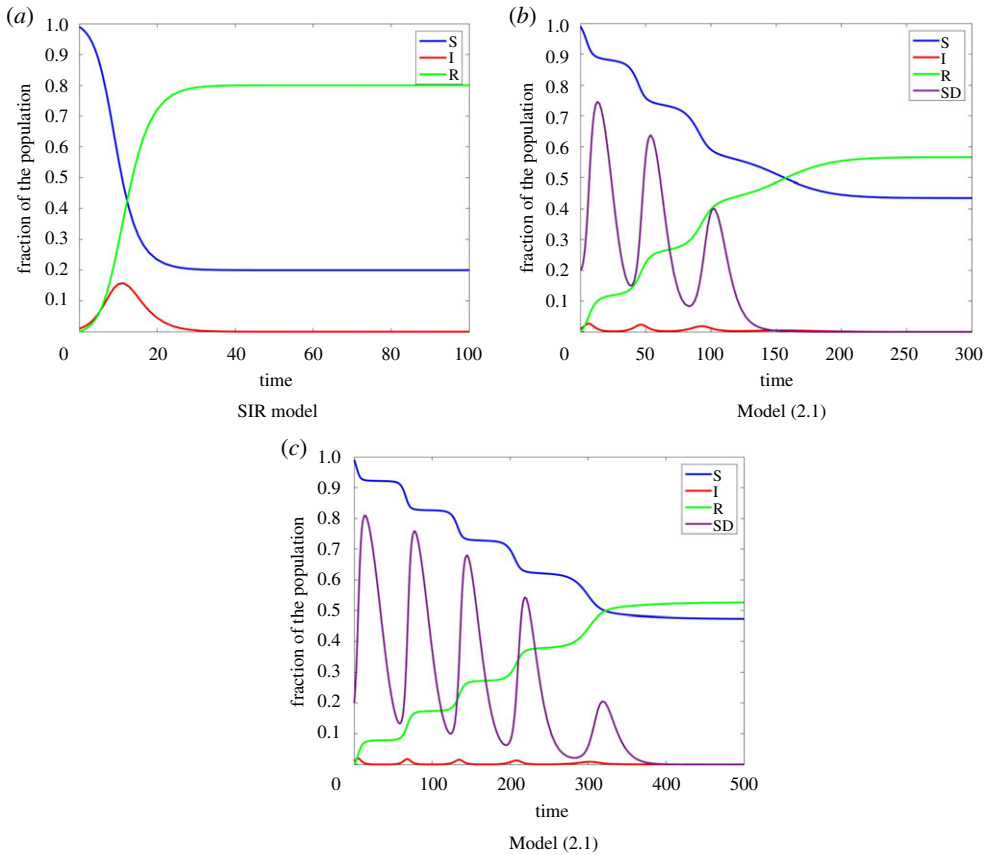
Figure 5. Comparison of the SIR model with Model (2.1) for $\beta = 0.8$, $\gamma = 0.4$ with $I_0 = 0.01$, $S_0 = 0.99$, $\mathcal{E}_0 = 0.2$, $C_{sd} = 0.75$ and (*b*) $C_I = 100$, $\omega = 1$, $\kappa = 2$, respectively (*c*) $C_I = 250$, $\omega = 0.5$, $\kappa = 0.5$. We clearly see here that social distancing reduces the total amount of infections. (Online version in colour.)

observe this in Model (2.1) as I oscillates around I^* with decreasing amplitude until the peak of the oscillations is smaller than I^* (figure 4).

(b) Social distancing saves lives

When comparing Model (2.1) to the SIR model, we immediately note that the total number of infections can be significantly smaller with social distancing (figure 5). Essentially, this means that voluntary social distancing can significantly reduce the total amount of infections $R(\infty)$. However, we also note that infections after the first wave of infection only emerge due to the *oscillatory tragedy of the commons*. If social distancing was practised until $I = 0$, we would have a much smaller $R(\infty)$.

Perfect adaption and Model (2.1) significantly reduce the total amount of infections compared to the SIR model. This is especially apparent for small I^* and slow adaption, i.e. small ω and κ. This is illustrated in figure 6.

Essentially, the explanation for this behaviour relates to herd immunity. Social distancing flattens the curve. Instead of one large wave of infections as in the SIR model, in Model (2.1) we can have several waves of infection with smaller peaks. An example of this is illustrated in figure 5. In the SIR model, herd immunity occurs if

$$S < \frac{\gamma}{\beta}.$$
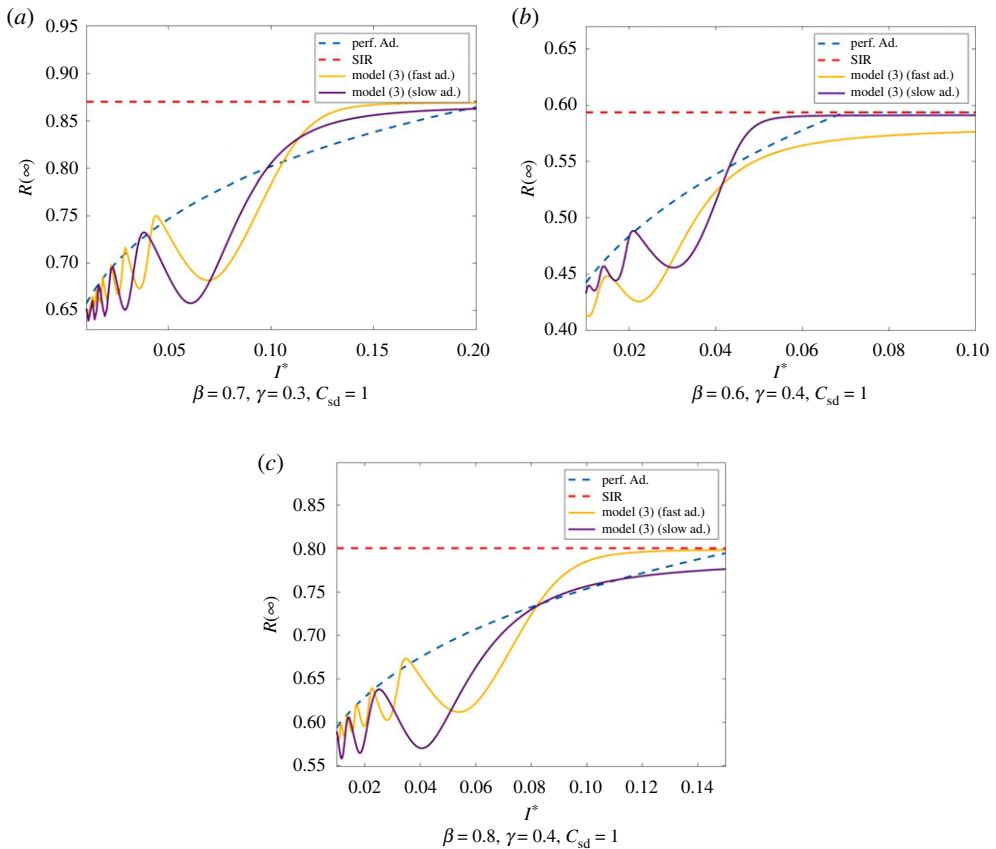
Figure 6. Comparison of the total number of infected for the SIR model, perfect adaption and Model (2.1) with initial values $I_0 = 0.01$, $S_0 = 0.99$, $\mathcal{E}_0 = 0.2$, and (a) $\omega = 1.5$ and $\kappa = 0.5$, respectively $\omega = 2$ and $\kappa = 1$, (b) $\omega = 1$ and $\kappa = 0.5$, respectively, $\omega = 1$ and $\kappa = 2$, (c) $\omega = 1$ and $\kappa = 0.5$, respectively $\omega = 1$ and $\kappa = 2$. Clearly, in perfect adaption and Model (2.1) the total amount of infections can be significantly smaller than in the SIR model. We see that also in Model (2.1) the amount of infections tends to grow if I^* grows. This will be discussed in §c. Moreover, small adaption parameters ω and κ in Model (2.1) can significantly reduce infections compared to perfect adaption as well as larger adaption parameters. This will be discussed in §d. (Online version in colour.)

Thus, I is increasing until $S = \gamma/\beta$ and then is monotonically decreasing. Even though, we have achieved some kind of herd immunity at this point, the high number of infected I still causes a high amount of new infections after herd immunity. Thus, the total amount of infections $R(\infty)$ is significantly larger than needed to obtain herd immunity. In Model (2.1), the dynamics are much more complicated. However, what remains as in the SIR model, is that as soon as (or at latest at this point) $S < \gamma/\beta$ the amount of infected I is monotonically decreasing, since then we have

$$\dot{I} = \beta(1 - \mathcal{E})SI - \gamma I \leq \beta SI - \gamma I < 0.$$

We denote the amount of infected when herd immunity is obtained by I_{HI}. With social distancing I_{HI} can become significantly smaller since social distancing significantly reduces the amount of infection. Other factors influencing the amount of new infection after herd immunity are the amount of recovered when herd immunity is achieved (denoted by R_{HI}) as well as the amount of people practising social distancing. R_{HI} can be much larger when social distancing is practised due to the spread of infections over a longer time period. People that practise social distancing further reduce the amount of new infections.
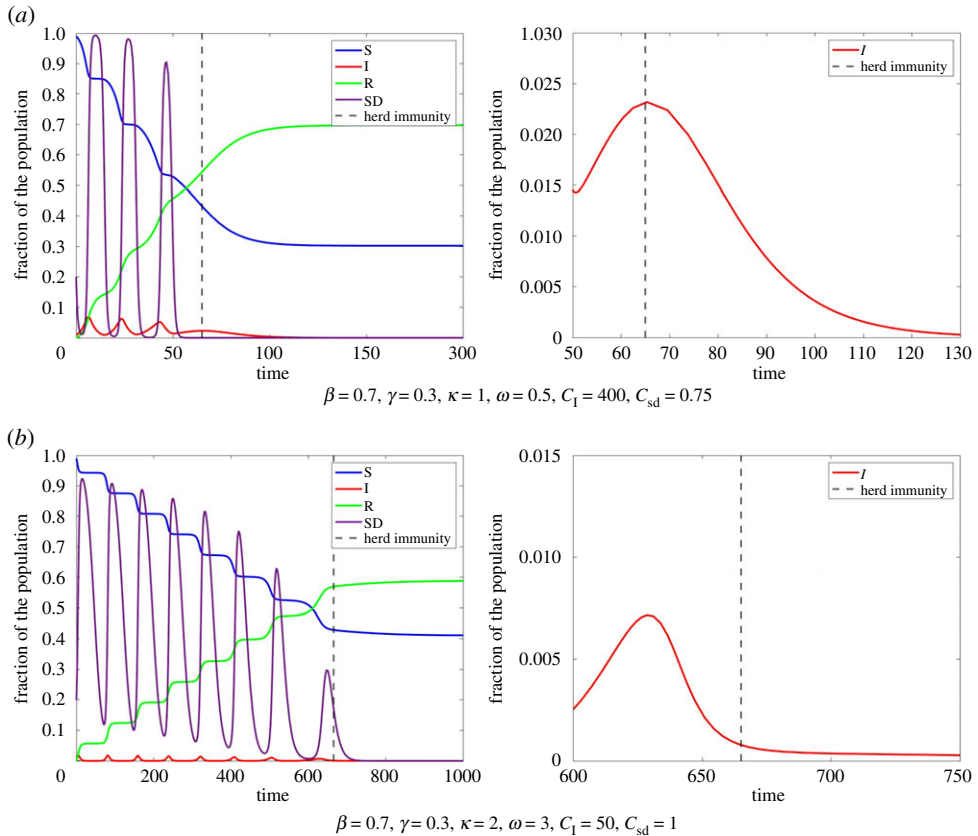
Figure 7. Occurrence of herd immunity for different parameters in Model (2.1). In both examples, herd immunity occurs for $S < \beta/\gamma$. However, for the parameters in (*a*), we have significantly less infected at this point than in (*b*). In (*a*), the small amount I_{HI} causes much less new infections than the larger I_{HI} in (*b*). Therefore, the total amount of infections for (*a*) is much smaller than for (*b*). (Online version in colour.)

Together, all these factors cause a significant decrease in new infections after herd immunity is achieved. Since small I_{HI} mostly coincides with large R_{HI} as well as high $\mathcal{E}$, we focus on I_{HI} here. When choosing the parameters $\omega, \kappa, C_{sd}, C_I$ such that I_{HI} is small, R_{HI} and many people practice social distancing, we can even achieve $R(\infty)$ to be near the herd immunity threshold $1 - \gamma/\beta$. For an illustration of this, see figure 7.

This also explains why perfect adaption causes larger total amounts of infections than Model (2.1). For perfect adaption, herd immunity is obtained for $t = t^*$ with $I = I^*$ while I_{HI} often is significantly smaller in Model (2.1). In particular, if we have $I > I^*$ while S is close to γ/β, small increases in $\mathcal{E}$ cause a decrease in I. Hence, $I_{HI} < I^*$ in most cases. For instance, in figure 7*a*, we have $I^* \approx 0.00268$ while I_{HI} can be much smaller in Model (2.1). However, we once again remember the *oscillatory tragedy of the commons*, i.e. that higher compliance to social distancing when I is small could lead to much smaller $R(\infty)$.

Next, we want to analyse how the perceived cost of social distancing C_{sd} as well as the perceived cost of infection C_I influence the total amount of infections $R(\infty)$.

(c) Larger cost of infection and smaller cost of social distancing reduce infections

As one might expect, if the cost of infection C_I increases or the cost of social distancing C_{sd} decreases, this induces an increase in the amount of people practising social distancing and thereby a decrease in infections. This behaviour becomes quite apparent in figure 8.
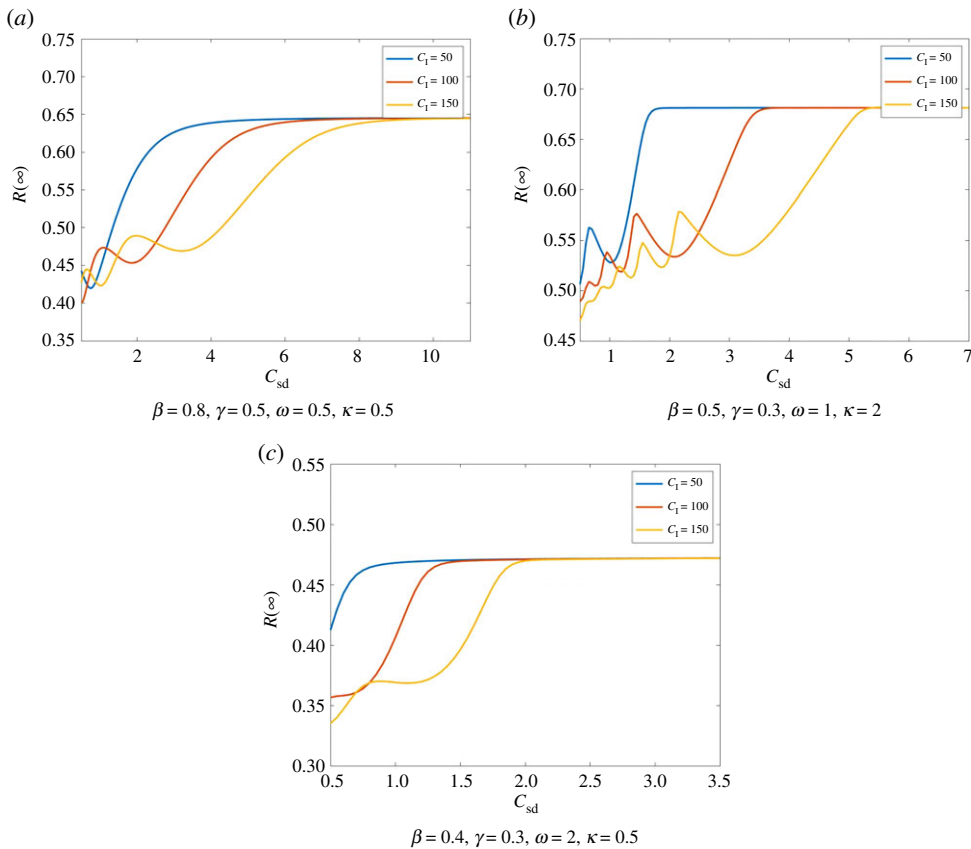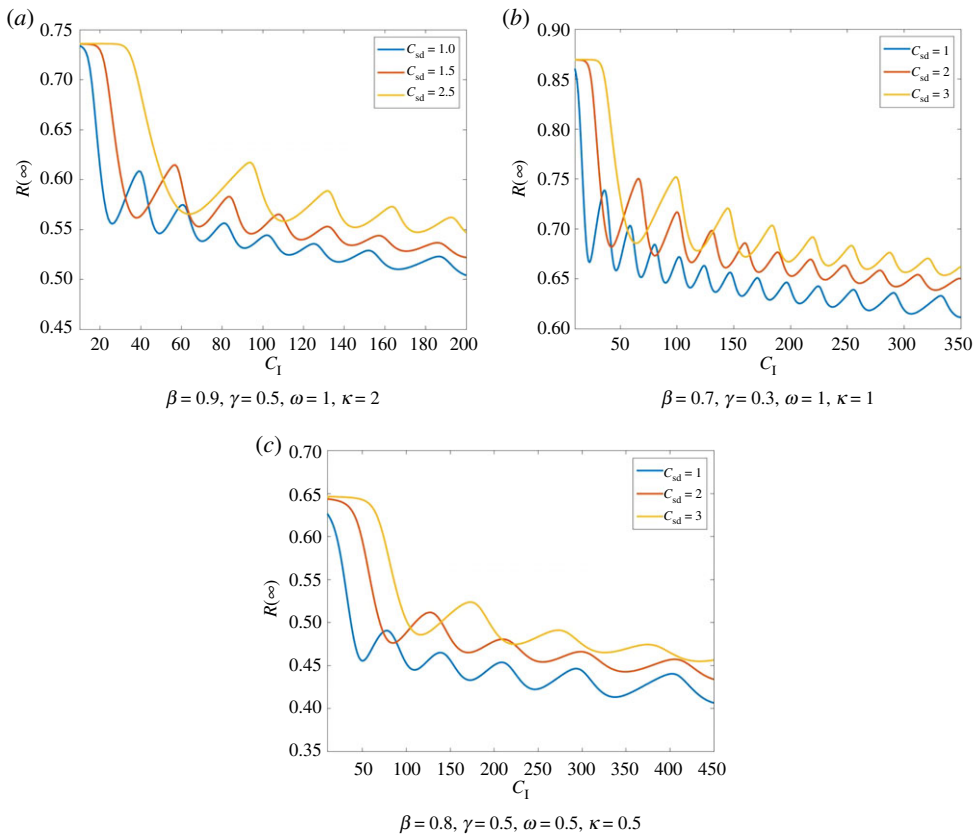
Figure 8. Total number of infections dependent of the cost of social distancing. We compare Model (2.1) for different costs of social distancing. Here, we have $I_0 = 0.01$, $S_0 = 0.99$, $\mathcal{E}_0 = 0.3$. In all three scenarios, we see that despite small oscillations in $R(\infty)$ the number of infections is overall increasing in C_{sd}. Moreover, we see that for large C_I the total number of infections can be significantly smaller, i.e. the tendency that higher costs of infection decrease the number of infections. Moreover, larger C_I as well as larger κ and ω cause a higher number of smaller oscillations. (Online version in colour.)

We can observe a similar tendency for C_I. Though, here we have larger oscillations in the total size of infections. These oscillations decrease in their amplitude and level off at $R_{PA}(\infty)$. An example for this behaviour can be seen in figure 9.

An explanation for this behaviour is connected to the observation made in §b that is illustrated in figure 7. To reduce $R(\infty)$, (among other factors) I_{HI} has to be small. One way to achieve this is to reduce I^*, the threshold that I oscillates around. Therefore, smaller C_{sd} as well as larger C_I tend to cause a decrease in $R(\infty)$. However, this does not yet explain how the oscillations occur. For this purpose, we have a look at figure 10. Here, we see that reducing I^* has two opposing effects on $R(\infty)$:

(i) A decrease in I^* causes a decrease in the size of the waves of infections and thus a decrease in I_{HI}. This causes a decrease in $R(\infty)$.

(ii) When decreasing I^* too much, this can lead to the development of a new wave of infections. When this occurs, we have an increase in I, before herd immunity is obtained. This causes a larger I_{HI}. Therefore, we have an increase in the total amount of infections $R(\infty)$ when a new wave of infections develops.

Figure 9. Total number of infections dependent of the cost of infection. We compare Model (2.1) for different costs of social distancing (with initial values $I_0 = 0.01$, $S_0 = 0.99$, $\mathcal{E}_0 = 0.2$). $R(\infty)$ shows oscillations with decreasing amplitude. These oscillations appear to be levelling of approximately at $R_{PA}(\infty)$. We see the tendency that $R(\infty)$ decreases for increasing C_I. Moreover, $R(\infty)$ is smaller here again for smaller C_{sd}. (Online version in colour.)
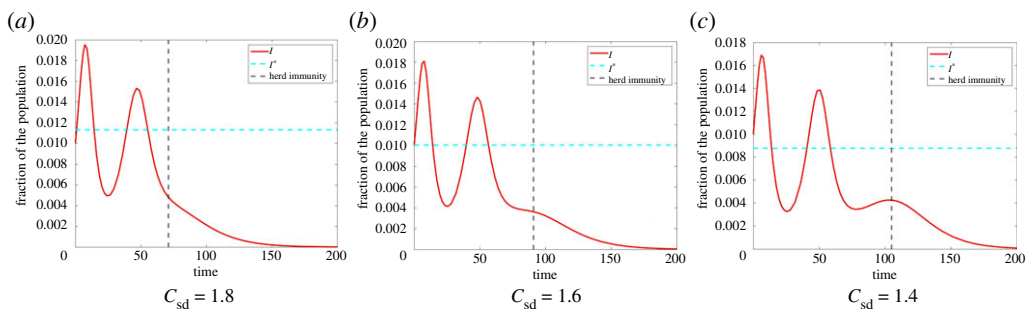
Figure 10. The amount of infected when herd immunity is obtained in Model (2.1) with $\beta = 0.8$, $\gamma = 0.5$, $\omega = 0.5$, $\kappa = 0.5$, $C_I = 200$, initial condition $I_0 = 0.01$, $S_0 = 0.99$, $\mathcal{E}_0 = 0.15$ and different C_{sd}. For (a) $C_{sd} = 1.8$, we have two waves of infection and herd immunity is obtained after approximately 70 days. We have $I_{HI} \approx 0.0045$ and overall we have a proportion of $R(\infty) \approx 0.4418$ infections. For (b) $C_{sd} = 1.6$, the waves of infection decrease in size. Thus, herd immunity is obtained after a longer period of time ($t = 90$). At the time, we get herd immunity, we have a smaller amount of infections ($I_{HI} \approx 0.0035$) and overall we have $R(\infty) \approx 0.4389$ infections. However, we see the beginning of the development of a third wave of infection. For (c) $C_{sd} = 1.4$, we see the effect of this third wave of infection. Herd immunity here is obtained after 105 days with an amount of infected $I_{HI} \approx 0.0042$. Even though, we have a smaller I^* here, the third wave of infection causes an increase in overall infections. Here, we have $R(\infty) \approx 0.4442$ and thus even more infections than for $C_{sd} = 1.8$. (Online version in colour.)
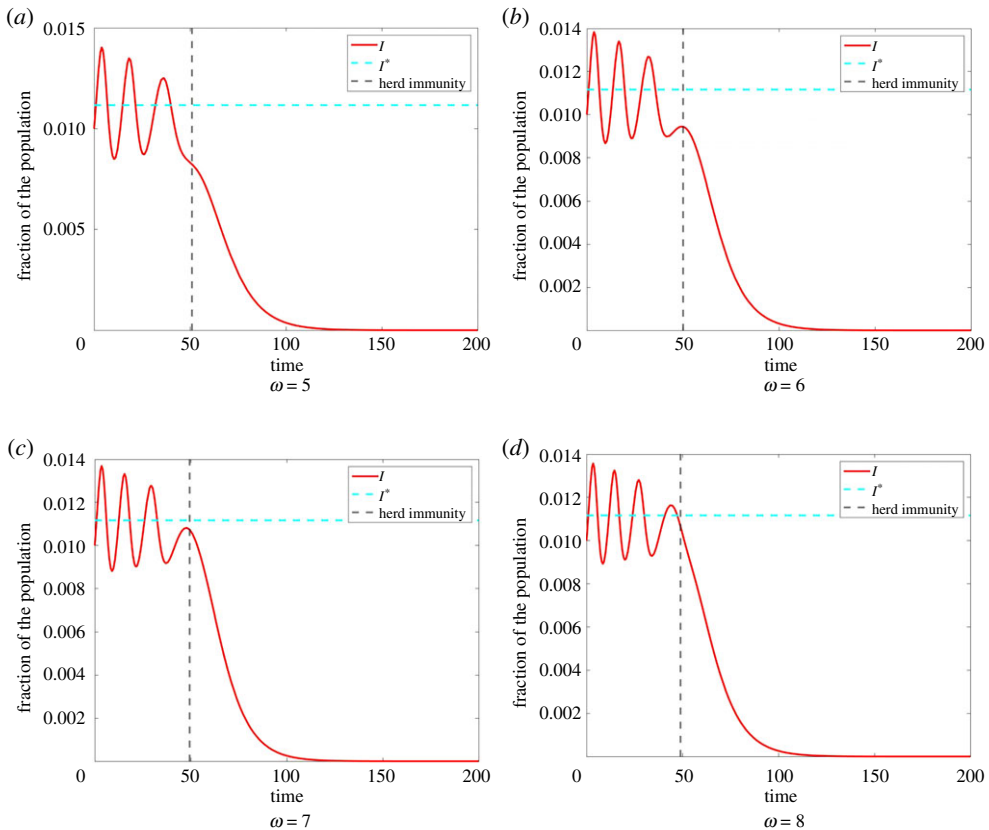
Figure 11. Development of an oscillation in the total number of infections. In Model (2.1) with $\beta = 0.9$, $\gamma = 0.6$, $\kappa = 0.5$, $C_I = 100$, $C_{sd} = 1$ and initial condition $I_0 = 0.01$, $\mathcal{E}_0 = 0.2$, we observe the amount of infected I. As can be seen in figure 12, $R(\infty)$ has a local minimum in this case approximately at $\omega = 5$. In (a), we have $\omega = 5$, herd immunity is achieved for $t \approx 50$ and at this time, we have $I_{HI} \approx 0.0083$. The total amount of infections is given by $R(\infty) \approx 0.4316$. For (b) $\omega = 6$ herd immunity is achieved at approximately the same time, with $II_{HI} \approx 0.0094$ and total amount of infections $R(\infty) \approx 0.4385$. For (c) $\omega = 7$ herd immunity is achieved at approximately the same time, with $I_{HI} \approx 0.0106$ and total amount of infections $R(\infty) \approx 0.4432$. Finally, for (c) $\omega = 8$ herd immunity is achieved at approximately the same time, with $I_{HI} \approx 0.0101$ and total amount of infections $R(\infty) \approx 0.4395$. For increasing ω, we observe that the first three waves of infection decrease in duration and intensity. However, a fourth wave of infection develops. This leads to an increase in the amount of infections when herd immunity is achieved and therefore an increase in the total amount of infections for $\omega = 6$, respectively, $\omega = 7$ compared to $\omega = 5$. For $\omega = 8$, however, herd immunity is only obtained after the fourth wave of infection is already decreasing again. Therefore, we have a decrease in the total amount of infections for $\omega = 8$ compared to $\omega = 7$. Note also that the amount of infected when herd immunity is achieved, is in all cases smaller than I^*. If we have $I > I^*$ while S is close to γ / β, small increases in $\mathcal{E}$ cause a decrease in I. Hence, I is mostly smaller than I^* when herd immunity occurs. This also induces that $R(\infty)$ is mostly smaller than $R_{PA}(\infty)$ as can also be seen in figure 12. (Online version in colour.)

This leads to the oscillations, that we observed in figure 9. When reducing C_{sd} we first see a decrease in $R(\infty)$ (caused by smaller waves of infection and a smaller I_{HI}) followed by an increase (induced by a new wave of infections that leads to an increase in I_{HI}).

(d) Faster responses and higher rationality increase infections

Two other important factors determining $R(\infty)$ are the responsiveness ω and the rationality parameter κ. In Model (2.1), a larger ω causes faster adaption of social distancing to the amount of infected. This has two opposing effects.
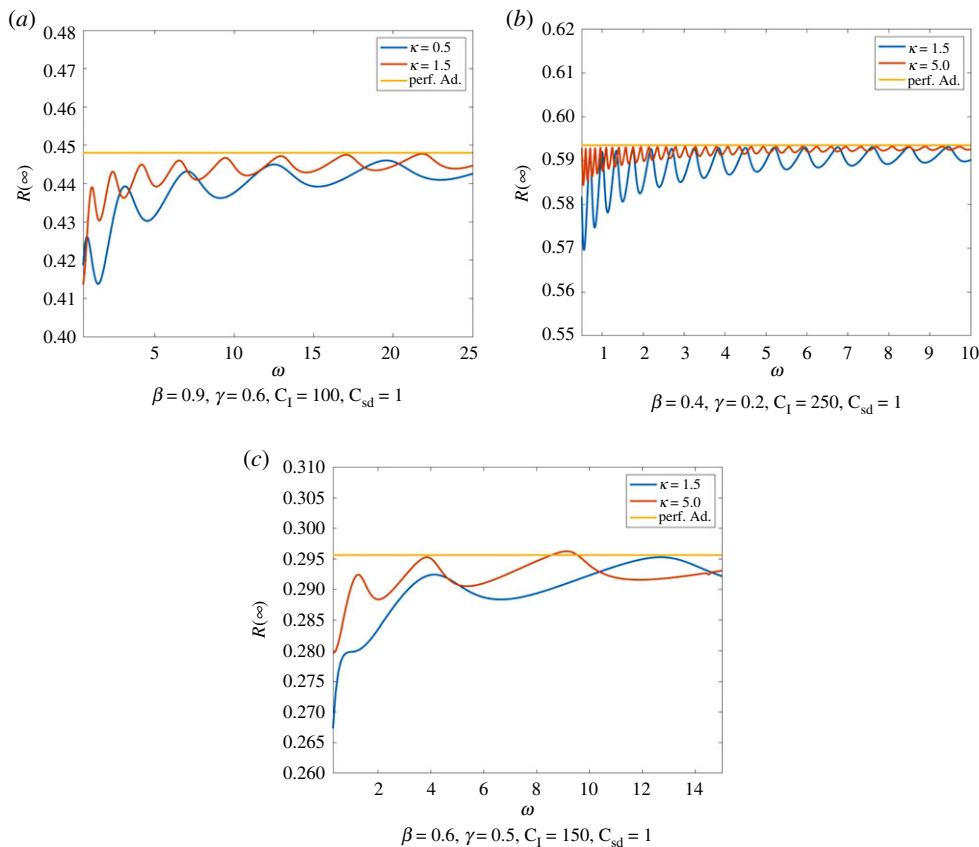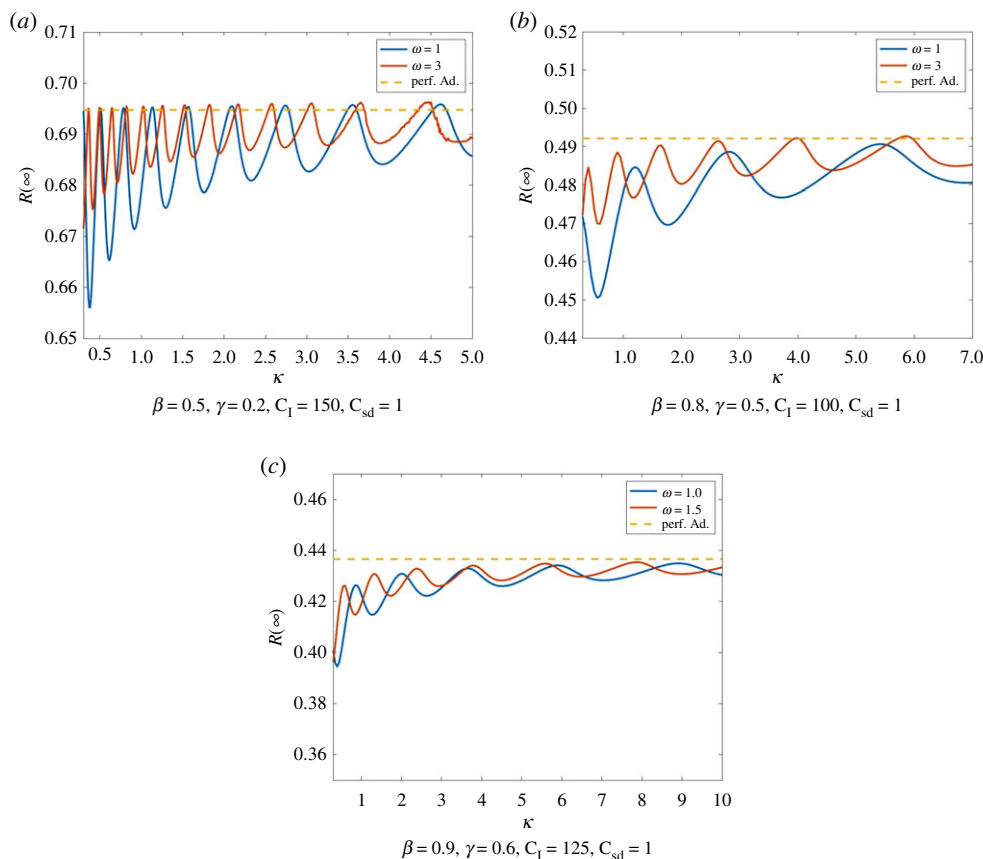
Figure 12. Total number of infections dependent of the responsiveness rate. We compare Model (2.1) for different rationality parameters with perfect adaption. Again, we have the initial condition $I_0 = 0.01$, $\mathcal{E}_0 = 0.2$. $R(\infty)$ shows oscillations with decreasing amplitude converging to perfect adaption here again for the same reasons as explained in §3c. This also explains the increasing number of oscillations for increasing κ and C_I. Moreover, $R(\infty)$ appears to be increasing for increasing ω, in particular, if κ and C_I are small. (Online version in colour.)

(i) On the one hand, faster adaptions causes a decrease in the duration of the waves of infection with smaller maxima and larger minima.

(ii) On the other hand, these smaller waves of infection can cause the development of another wave of infection. In particular, if herd immunity is obtained before this new wave recedes, this leads to an increase in I_{HI}. Thus, leading to an increase of infections.

Overall, we thus have oscillations in $R(\infty)$ depending on ω. An example of this is illustrated in figure 11.

With increasing ω the deviations of I from I^* are decreasing due to faster adaption. This leads to a decrease in the amplitude of the oscillations in $R(\infty)$ and to $R(\infty)$ levelling off approximately at $R_{\mathrm{PA}}(\infty)$. As explained before, we mostly have $I_{\mathrm{HI}} < I^*$. Therefore, larger deviations from perfect adaption where $I_{\mathrm{HI}} = I^*$ cause a decrease in $R(\infty)$. An example of this behaviour is illustrated in figure 12.

The rationality parameter κ has a nearly similar effect as ω on the dynamics of our model. In Model (2.1), a large rationality parameter κ means that individuals change their strategy as soon as the payoff of infection becomes larger than the payoff of social distancing and vice versa. Therefore, large κ induce faster adaption of $\mathcal{E}$ and therefore smaller oscillations of I around I^*. An increase in κ thus causes a decrease in the duration in the waves of infection as well as smaller

Figure 13. Total number of infections dependent of the rationality parameter. We compare Model (2.1) with initial condition $I_0 = 0.01$, $\mathcal{E}_0 = 0.2$ for different responsiveness rates with perfect adaption. Again, we observe the same kind oscillations in $R(\infty)$ that are caused by the development of new waves of infection. Smaller responsiveness parameters ω cause smaller oscillations and tendentially fewer infections. (Online version in colour.)

maxima and larger minima. Hence, a change in κ has a similar effect on $R(\infty)$ as a change in ω. Here as well, we have oscillations caused by the development of new waves of infection, that are decreasing and levelling off at $R_{\mathrm{PA}}(\infty)$. Thus, $R(\infty)$ tends to decrease for smaller κ (figure 13).

4. Discussion and conclusion

Social distancing is often used in combination with other control measures such as mask wearing, and testing and isolation. It is worthy of further investigation to account for individual preferences in their adoption choices when multiple interventions for disease mitigation are available. Generally speaking, individuals become less vigilant and feel less need to follow disease intervention measures suggested by public health officials, if the epidemic curve is being bent down, but as a result, the uptick of cases in turn causes individuals to increase their compliance levels. The feedback loop of this sort gives rise to an oscillatory dynamics of behavioural compliance and disease prevalence, as reported in the present work. Similar phenomena have previously been studied in the context of eco-evolutionary dynamics where the payoff structure of individual interactions can be regulated by the environmental feedback [43–45].

Social distancing can be regarded as an altruistic behaviour that incurs a cost to oneself but collectively benefits other community members especially these vulnerable in the population.

Thus monetary or non-monetary means can be used to incentivize non-compulsory social distancing. For example, during the COVID-19 health crisis, governments have subsidized the cost of staying at home through tax reduction or other stimulus packages for both workers and their employers [28]. Besides, an individual who opts for social distancing can create a positive psychological reward, which in fact reduces the perceived overall cost of social distancing. As shown in several experimental works [46–48], encouraging altruistic social distancing, especially if people can afford to do so, through promoting a strong sense of community, empathy and compassion [49], can lead to desired compliance of social distancing. In this sense, promoting human cooperation in the social dilemma of disease control is a new promising direction for future work.

While our proof-of-principle model offers enlightening insights into understanding compliance issues in the dilemma of social distancing, *targeted* social distancing can be investigated by further accounting for individual heterogeneity as the attack rate and mortality rate of infectious diseases, such as the influenza [50,51] and the COVID-19 pandemic [52], are age-dependent. Thus, extending our model with an age structure will be useful to quantify the heterogeneity in both the risk of infections and the cost of social distancing for each age group. This consideration parameterized using realistic contact mixing matrices in a social network [53] as well as with an age structure (more generally, multilayer networks [54]) can be used to optimize social network-based distancing protocol (targeted social distancing) [34]. Further work along this direction is promising and will help provide practical guidance. Moreover, it appears that instead of the actual likelihood to get infected, one's perceived likelihood to get infected influences the decision whether to engage in social distancing and face covering [46]. Variation in individual risk assessment might therefore influence the results in our model and be an interesting extension to the model in future work.

In sum, we analyse and characterize oscillatory dynamics in the dilemma of social distancing, which arises from the non-trivial feedback between disease prevalence and behavioural intervention. Our results suggest an *oscillatory tragedy of the commons* in disease control when individuals act in their own right without coordination or in the absence of centralized institutions to enforce their compliance, a phenomenon that has been observed in past pandemics like the Spanish flu [55] and seems to repeat in the current COVID-19 pandemic [56]. Our work provides new insight into the dual role of human behaviour that can fuel, or fight against, the pandemic [57]. To resolve the dilemma of disease control from global pandemics to resurgence of common diseases (like measles which has become endemic in some regions [58]), a deep understanding of pertinent behavioural aspect in disease control and prevention, and large-scale human cooperation in particular, is urgently needed and will help to better inform pandemic support in the future [49].

References

1. Petersen LR, Jamieson DJ, Powers AM, Honein MA. 2016 Zika virus. *N. Engl. J. Med.* **374**, 1552–1563. (doi:10.1056/NEJMra1602113)

2. Leroy EM, Kumulungui B, Pourrut X, Rouquet P, Hassanin A, Yaba P, Délicat A, Paweska JT, Gonzalez J, Swanepoel R. 2005 Fruit bats as reservoirs of Ebola virus. *Nature* **438**, 575–576. (doi:10.1038/438575a)

3. Andersen KG, Rambaut A, Lipkin W, Holmes EC, Garry RF. 2020 The proximal origin of SARS-CoV-2. *Nat. Med.* **26**, 450–452. (doi:10.1038/s41591-020-0820-9)

4. Lloyd-Smith JO. 2017 Infectious diseases: predictions of virus spillover across species. *Nature* **546**, 603–604. (doi:10.1038/nature23088)

5. Bauch CT, Galvani AP. 2013 Social factors in epidemiology. *Science* **342**, 47–49. (doi:10.1126/science.1244492)

6. Verelst F, Willem L, Beutels P. 2016 Behavioural change models for infectious disease transmission: a systematic review (2010–2015). *J. R. Soc. Interface* **13**, 20160820. (doi:10.1098/rsif.2016.0820)

7. Fu F, Rosenbloom DI, Wang L, Nowak MA. 2011 Imitation dynamics of vaccination behaviour on social networks. *Proc. R. Soc. B* **278**, 42–49. (doi:10.1098/rspb.2010.1107)

8. Reluga TC, Bauch CT, Galvani AP. 2006 Evolving public perceptions and stability in vaccine uptake. *Math. Biosci.* **204**, 185–198. (doi:10.1016/j.mbs.2006.08.015)

9. Wang Z, Bauch CT, Bhattacharyya Sa, Manfredi P, Perc M, Perra N, Salathé M, Zhao D. 2016 Statistical physics of vaccination. *Phys. Rep.* **664**, 1–113. (doi:10.1016/j.physrep.2016.10.006)

10. Bauch CT, Bhattacharyya S. 2012 Evolutionary game theory and social learning can determine how vaccine scares unfold. *PLoS Comput. Biol.* **8**, e1002452. (doi:10.1371/journal.pcbi.1002452)

11. Wang W, Liu Q, Cai S, Tang M, Braunstein LA, Stanley HE. 2016 Suppressing disease spreading by using information diffusion on multiplex networks. *Sci. Rep.* **6**, 29259.

12. Salathé M, Bonhoeffer S. 2008 The effect of opinion clustering on disease outbreaks. *J. R. Soc. Interface* **29**, 1505–1508. (doi:10.1098/rsif.2008.0271)

13. Funk S, Salathé M, Jansen VAA. 2010 Modelling the influence of human behaviour on the spread of infectious diseases: a review. *J. R. Soc. Interface* **7**, 1247–1256. (doi:10.1098/rsif.2010.0142)

14. Fenichel EP *et al.* 2011 Adaptive human behavior in epidemiological models. *Proc. Natl Acad. Sci. USA* **108**, 6306–6311. (doi:10.1073/pnas.1011250108)

15. Fu F, Christakis NA, Fowler JH. 2017 Dueling biological and social contagions. *Sci. Rep.* **7**, 43634. (doi:10.1038/srep43634)

16. Chen X, Fu F. 2019 Imperfect vaccine and hysteresis. *Proc. R. Soc. B* **286**, 20182406. (doi:10.1098/rspb.2018.2406)

17. Bauch CT. 2005 Imitation dynamics predict vaccinating behaviour. *Proc. R. Soc. B* **272**, 1669–1675. (doi:10.1098/rspb.2005.3153)

18. Arefin MR, Masaki T, Tanimoto J. 2020 Vaccinating behaviour guided by imitation and aspiration. *Proc. R. Soc. A* **476**, 20200327. (doi:10.1098/rspa.2020.0327)

19. Cressman R, Tao Y. 2014 The replicator equation and other game dynamics. *Proc. Natl Acad. Sci. USA* **111**, 10810–10817. (doi:10.1073/pnas.1400823111)

20. Sigmund K, Hauert C, Nowak MA. 2001 Reward and punishment. *Proc. Natl Acad. Sci. USA* **98**, 10 757–10 762. (doi:10.1073/pnas.161155698)

21. Perc M, Jordan JJ, Rand DG, Wang Z, Boccaletti S, Szolnoki A. 2017 Statistical physics of human cooperation. *Phys. Rep.* **687**, 1–51. (doi:10.1016/j.physrep.2017.05.004)

22. Page KM, Nowak MA, Sigmund K. 2000 The spatial ultimatum game. *Proc. R. Soc. Lond. B* **267**, 2177–2182. (doi:10.1098/rspb.2000.1266)

23. Capraro V, Perc M, Vilone D. 2020 The evolution of lying in well-mixed populations. *J. R. Soc. Interface* **16**, 20190211. (doi:10.1098/rsif.2019.0211)

24. Kumar A, Capraro V, Perc M. 2020 The evolution of trust and trustworthiness. *J. R. Soc. Interface* **17**, 20200491. (doi:10.1098/rsif.2020.0491)

25. Capraro V, Perc M. 2019 Grand challenges in social physics: in pursuit of moral behavior. *Front. Phys.* **6**, 107. (doi:10.3389/fphy.2018.00107)

26. Chen X, Fu F. 2018 Social learning of prescribing behavior can promote population optimum of antibiotic use. *Front. Phys.* **6**, 139. (doi:10.3389/fphy.2018.00139)

27. Townsend AK, Hawley DM, Stephenson JF, Williams KE. 2020 Emerging infectious disease and the challenges of social distancing in human and non-human animals. *Proc. R. Soc. B* **287**, 20201039. (doi:10.1098/rspb.2020.1039)

28. Nicola M, Alsafi Z, Sohrabi C, Kerwan A, Al-Jabir A, Iosifidis C, Agha M, Agha R. 2020 The socio-economic implications of the coronavirus and COVID-19 pandemic: a review. *Int. J. Surg.* **78**, 185–193.

29. Reluga TC. 2010 Game theory of social distancing in response to an epidemic. *PLoS Comput. Biol.* **6**, e1000793. (doi:10.1371/journal.pcbi.1000793)
30. Maharaj S, Kleczkowski A. 2012 Controlling epidemic spread by social distancing: do it well or not at all. *BMC Public Health* **12**, 679. (doi:10.1186/1471-2458-12-679)
31. Huberts N, Thijssen J. 2020 Optimal Timing of Interventions during an Epidemic. *Available at SSRN 3607048*.
32. Caley P, Philp DJ, McCracken K. 2008 Quantifying social distancing arising from pandemic influenza. *J. R. Soc. Interface* **5**, 631–639. (doi:10.1098/rsif.2007.1197)
33. Wallinga J, van Boven M, Lipsitch M. 2010 Optimizing infectious disease interventions during an emerging epidemic. *Proc. Natl Acad. Sci. USA* **107**, 23–928. (doi:10.1073/pnas.0908491107)
34. Aleta A *et al.* 2020 Modelling the impact of testing, contact tracing and household quarantine on second waves of COVID-19. *Nat. Hum. Behav.* **4**, 964–971.
35. Kissler SM, Tedijanto C, Goldstein E, Grad YH, Lipsitch M. 2020 Projecting the transmission dynamics of SARS-CoV-2 through the postpandemic period. *Science* **368**, 860–868. (doi:10.1126/science.abb5793)
36. Sethi SP, Staats PW. 1978 Optimal control of some simple deterministic epidemic models. *J. Oper. Res. Soc.* **29**, 129–136. (doi:10.1057/jors.1978.27)
37. Abakuks A. 1974 Optimal immunisation policies for epidemics. *Adv. Appl. Probab.* **6**, 494–511. (doi:10.2307/1426230)
38. Abakuks A. 1973 An optimal isolation policy for an epidemic. *J. Appl. Probab.* **10**, 247–262. (doi:10.2307/3212343)
39. Wickwire KH. 1975 Optimal isolation policies for deterministic and stochastic epidemics. *Math. Biosci.* **26**, 325–346. (doi:10.1016/0025-5564(75)90020-6)
40. Morris DH, Rossine FW, Plotkin JB, Levin SA. 2020 Optimal, near-optimal, and robust epidemic control. (http://arxiv.org/abs/2004.02209)
41. Simon HA. 1990 Bounded rationality. In *Utility and probability* pp. 15–18. New York, NY: Springer.
42. Tversky A, Kahneman D. 1992 Advances in prospect theory: cumulative representation of uncertainty. *J. Risk Uncertain.* **5**, 297–323. (doi:10.1007/BF00122574)
43. Weitz JS, Eksin C, Paarporn K, Brown SP, Ratcliff WC. 2016 An oscillating tragedy of the commons in replicator dynamics with game-environment feedback. *Proc. Natl Acad. Sci. USA* **113**, E7518–E7525. (doi:10.1073/pnas.1604096113)
44. Tilman AR, Plotkin JB, Akçay E. 2020 Evolutionary games with environmental feedbacks. *Nat. Commun.* **11**, 1–11. (doi:10.1038/s41467-020-14531-6)
45. Wang X, Zheng Z, Fu F. 2020 Steering eco-evolutionary game dynamics with manifold control. *Proc. R. Soc. A* **476**, 20190643. (doi:10.1098/rspa.2019.0643)
46. Capraro V, Barcelono H. 2020 The effect of messaging and gender on intentions to wear a face covering to slow down COVID-19 transmission. *J. Behav. Econ. Policy* **4**, 45–55.
47. Jordan JJ, Yoeli E, Rand DG. 2020 Don't get it or don't spread it? Comparing self-interested versus prosocial motivations for COVID-19 prevention behaviors. (http://arxiv.org/abs/10.31234/osf.io/yuq7x)
48. Van Bavel J *et al.* 2020 National identity predicts public health support during a global pandemic. (http://arxiv.org/abs/10.31234/osf.io/ydt95)
49. Van Bavel JJ *et al.* 2020 Using social and behavioural science to support COVID-19 pandemic response. *Nat. Hum. Behav.* **4**, 460–471.
50. Apolloni A, Poletto C, Colizza V. 2013 Age-specific contacts and travel patterns in the spatial spread of 2009 H1N1 influenza pandemic. *BMC Infect. Dis.* **13**, 176. (doi:10.1186/1471-2334-13-176)
51. Eames, KDT, Tilston NL, Brooks-Pollock E, Edmunds WJ. 2012 Measured dynamic social contact patterns explain the spread of H1N1v influenza. *PLoS Comput. Biol.* **8**, e1002425. (doi:10.1371/journal.pcbi.1002425)
52. Wu JT, Leung K, Bushman M, Kishore N, Niehus R, de Salazar PM, Cowling BJ, Lipsitch ML, Leung GM. 2020 Estimating clinical severity of COVID-19 from the transmission dynamics in Wuhan, China. *Nat. Med.* **26**, 506–510. (doi:10.1038/s41591-020-0822-7)
53. Block P, Hoffman M, Raabe IJ, Dowd JB, Rahal C, Kashyap R, Mills MC. 2020 Social network-based distancing strategies to flatten the COVID-19 curve in a post-lockdown world. *Nat. Hum. Behav.* **4**, 583–596.
54. Aleta A, de Arruda GF, Moreno Y. 2020 Data-driven contact structures: from homogeneous mixing to multilayer networks. (http://arxiv.org/abs/2003.06946)

55. Taubenberger JK, Morens DM. 2006 1918 Influenza: the mother of all pandemics. *Emerg. Infect. Dis.* **12**, 15–22. (doi:10.3201/eid1209.05-0979)
56. Alwan NA *et al.* 2020 Scientific consensus on the COVID-19 pandemic: we need to act now. *Lancet* **396**, e71–e72. (doi:10.1016/S0140-6736(20)32153-X)
57. 2020 Behaviour fuels, and fights, pandemics. See https://www.nature.com/articles/s41562-020-0892-z (accessed on 24 June 2020).
58. Muscat M *et al.* 2009 Measles in Europe: an epidemiological assessment. *Lancet* **373**, 383–389. (doi:10.1016/S0140-6736(08)61849-8)

18

royalsocietypublishing.org/journal/rspa   *Proc. R. Soc. A* **476**: 20200686